ARTÍCULO DE INVESTIGACIÓN ORIGINAL

REVISTA MEXICANA DE INGENIERÍA BIOMÉDICA
SOMIB
Vol. XXXII, Núm. 2
Diciembre 2011
pp 125 - 132

Trabecular bone: texture analysis in CT to improve osteoporosis diagnosis in Duchenne muscle distrophy patients

Norma Pilar Castellanos Abrego*
Elisa Martínez Coria**
Josefina Gutierrez Martínez***

* Electrical Department, Universidad Autónoma Metropolitana-Iztapalapa, México City
** Division of Imagenology-Computed Tomography, Instituto Nacional de Rehabilitación, México City
*** Department of Technological Research, Instituto Nacional de Rehabilitación, México City

Correspondence:
Norma Pilar Castellanos Abrego,
e-mail: npca@xanum.uam.mx
Universidad Autonoma Metropolitana-Iztapalapa
Av. San Rafael Atlixco #186, Col. Vicentina, CP. 09340, Mexico City, México
tel: (55) 58044903

Received article: 28/junio/2011
Accepted article: 19/noviembre/2011

ABSTRACT

In recent years, interest in bone mineral densitometry (BMD) for children has increased, mainly due to the varieties of disease that influence bone growth. Trabecular bone densitometry in CT from lumbar vertebra is usually used clinically as a good indicator of bone deterioration and fracture risk. Nevertheless, diagnosing osteoporosis in obese and Duchenne Muscle Distrophy (DMD) children by BMD has been difficult due to the attenuation of radiation dose by abdominal fat, which could lead to overestimation of the degree of bone deterioration. The present work is an effort to improve pediatric osteoporosis diagnostic efficacy by analyzing the trabecular bone texture via CT with two frequency based methods: fractal dimension with power spectrum (D_{ps}) and wavelet packets (WP). Healthy young adults group in the peak bone mass was statistically compared (t-student) with osteoporotic women with either fractal dimension or the four WP energy bands, and the results suggested significant differences. Applying ANOVA to three DMD children groups classified by their z-score as having normal, low and very low bone mineral density, significant differences were also found. At last, when comparing the DMD pediatric groups with that osteoporotic women, great statistical significance was found for all texture indicators. Results shown that the introduced techniques for image texture analysis could quantify the trabecular bone deterioration; this may help to improve the osteoporosis diagnosis in overweight patients, in specific DMD children, where it is often a diagnostic challenge.

Key Words: Bone mineral densitometry, computed tomography, osteoporosis diagnosis, muscle dystrophy patients.

RESUMEN

En años recientes, el interés en el estudio de la densitometría mineral de hueso (DMH) para aplicaciones pediátricas se ha incrementado, debido principalmente a la variedad de enfermedades que influyen en el crecimiento del hueso. La densitometría del hueso trabecular en tomografía computada (TC) para vértebras lumbares se utiliza regularmente en la clínica como un buen indicador del deterioro del hueso y el riesgo de fractura. Sin embargo, el diagnóstico de la osteoporosis en pacientes pediátricos obesos y la distrofia muscular de Duchenne (DMD) por el método de DMH ha sido difícil debido a la atenuación de la dosis de radicación por la grasa abdominal, la cual puede producir la sobre estimación del grado de deterioro del hueso. El presente trabajo es un esfuerzo para mejorar la eficiencia del

diagnóstico de la osteoporosis pediátrica a través del análisis de la textura del hueso trabecular utilizando la TC con dos métodos basados en frecuencia: la dimensión fractal con el espectro de potencia (DEP) y paquetes wavelet (PW). Un grupo de pacientes adultos jóvenes en la masa pico del hueso fue estadísticamente comparada (prueba de t-student) con mujeres con osteoporosis que presentaban ya sea una dimensión fractal o las cuatro bandas de energía de los PW. Los resultados mostraron diferencias significativas. El método de ANOVA fue aplicado a los tres grupos de niños con DMH utilizando sus índices Z teniendo densidad mineral del hueso normal, baja y muy baja, mostrando diferencias significativas. Finalmente, cuando se compararon los grupos pediátricos afectados por DMH con mujeres afectadas por osteoporosis, una diferencia muy significativa fue encontrada para todos los indicadores de textura. Los resultados mostraron que las técnicas introducidas en este estudio para el análisis de imágenes de textura puede cuantificar el deterioro del hueso trabecular. Esto podría ayudar para mejorar el diagnóstico de la osteoporosis en pacientes con sobrepeso, en niños específicos con DMH que en general es un reto médico importante.

Palabras clave: Densitometría mineral de hueso, tomografía computada, diagnóstico de osteoporosis, pacientes de distrofia muscular

INTRODUCTION

Osteoporosis is a progressive condition in which bone density is lost or there is insufficient bone formation, thereby weakening the bones and making them more susceptible to fractures. Although it is much more common in adults (especially menopausal and post-menopausal women), osteoporosis can also occur during childhood or young adulthood. Osteoporosis during childhood is most frequently caused by an underlying medical condition or a genetic disorder, such as osteogenesis imperfecta, leukemia, nutritional deficiencies, or corticosteroid use[1]. Histologically, it appears as thinning and increased porosity of cortices and a reduction in the size and number of trabecula.

Bone mineral density (BMD) is a medical term referring to the amount of matter per cubic centimeter of bones. BMD is used in clinical medicine as an indirect indicator of osteoporosis and fracture risk. In adults, diagnosing osteoporosis or osteopenia is performed by a T-score –a comparison of the patient's BMD with an adult in his peak bone mass (typically a Caucasian male 20 years of age). This method is inappropriate to diagnose osteoporosis in children. Diagnosis in children should be performed on the basis of a Z-score that compares the patient with others of the same age, sex and ethnicity[2].

In recent years, interest in bone densitometry for children has increased, mainly due to the varieties of disease that influence bone growth. Nevertheless, one should consider that, until now, all bone densitometry techniques have been exclusively designed, developed and validated for use in an adult population[3].

Dual-energy X-ray Absorptiometry (DXA) is the preferred method of assessing bone mineral status in clinical practice because of its speed, precision and low radiation exposure. Unfortunately, the acquisition and interpretation of DXA data in growing children is more complex than in adults. In addition, DXA only provides a two-dimensional measurement of the three-dimensional skeleton[4,5].

Quantitative Computed Tomography (QCT) should be the gold standard in bone densitometry because it assesses bone mass as a volume. In QCT, the Hounsfield unit of a specific voxel is compared with a phantom scanned within the same field of view; this yields the BMD expressed as grams of CaHaP/cm^3. In addition, as a true volumetric bone densitometry technique, QCT is also capable of separating cortical and trabecular bone. On the other hand, a major disadvantage is the higher radiation dose, compared with DXA. Previously, to our knowledge, only Gilsanz et al[2], van Rijn et al[3] and Friecke et al[6], have reported the use of QCT in large pediatric study groups.

It is recognized that physical activity, dietary intake, and hereditary also affect BMD[7] but another problem is obesity. Reports demonstrate that the number of radiology studies that were considered difficult to interpret as a result of patient obesity has

doubled over the last 15 years. To obtain quality CT images in obese patients, a KVP of at least 140 is necessary to penetrate through the adipose tissue[8]. In another study with phantoms and dosimeters[9], it was found that a greater percentage increase in skin dose is needed as patient size increases. An explanation may be the greater attenuation of the traversing photon through abdominal fat, resulting in lower detection of radiation by the center compared with the body surface. The radiation dose increases for increased subcutaneous fat thicknesses[10].

Concurrently, positive results and side effects of long-term steroid treatment, such as obesity, have been observed for Duchenne muscular dystrophy patients and are characterized by progressive muscle degeneration and substitution with fat and connective tissue[11,12]. In addition, osteopenia has been described in a variety of pathological, traumatic conditions in which the continuous weight-bearing stimulus is missing or reduced in the critical period of childhood and adolescence[13,14].

Currently, physicians must use good clinical judgment in the management of young patients at risk of bone fragility. Due to the problems mentioned above, the present work is an effort to improve osteoporosis diagnosis in children by analyzing the trabecular bone texture in CT.

Tools for diagnosing osteoporosis using texture analysis by fractal dimension began with the exploration of alveolar dental bone radiographies. The objectives of this investigation were to study radiographic pattern changes in areas of interdental human maxillary alveolar bone during simulated osteoporosis. This work concludes that the fractal dimension by the spectral power spectrum decreases during simulated osteoporosis. Although trabecular bone from lumbar vertebras has been considered a better site for studying bone microarchitecture in pediatric patients, this work is one of the first that correlates bone osteoporosis with the fractal dimension[15].

Other authors use fractal analysis to extract the features from trabecular bone x-ray images. Here, they estimate global and directional fractal dimensions from thick sections and compare the ability of the Minkowski dimension and power spectrum to characterize bone textures using bovine femurs and tibias from x-ray images[16].

Mathematical morphology is also used to compute the fractal dimension of bone x-rays of rats using the distal end of the femur. They concluded that this method can be a useful indicator in the early prediction of diseases such as osteoporosis[17].

The wavelet transform has been commonly applied to texture analysis as an important multiresolution analysis tool[18,19]. To our knowledge, it has not yet been applied to trabecular bone for diagnosing osteoporosis. One prior report contributed to computer-aided diagnosis, but it is focused on breast cancer[20].

The present work performs an analysis of trabecular bone texture in osteoporotic women and compares it with healthy women in their peak bone mass and DMD children. This is motivated by the problems in diagnosing osteoporosis in DMD children, among whom low BMD is common. Two different methods of texture analyses based on spatial frequencies are proposed to make this task: fractal dimension using power spectrum and wavelet packets. A review of these methods is described in the next section.

METHODOLOGY

Subjects in this study are a compilation of healthy young adults, elderly woman with osteoporosis diagnose and Duchenne Muscle Distrophy (DMD) children at Instituto Nacional de Rehabilitación (INR) in México City, México. All subjects were assessed with a quantitative CT scanner (GE Light Speed V-CT at 120 KVP, 120 mA, and 5 mm of thickness) with the same mineral reference phantom (0, 125, and 250 mg/cm^3 solid hydroxyapatite equivalent) for simultaneous calibration (CT-T bone densitometry software, GE Medical Systems). The sites to be scanned were identified with lateral scout views using a L2-L4 lumbar spine for measurement of BMD[21]. Image spatial resolution of 512 x 512 pixels was obtained.

BMDs were obtained for all subjects by the mean value of the three lumbar vertebras. The Region of Interest (ROI) was detected automatically in the trabecular bone by the commercial software. In texture analysis, ROIs were identified manually in the same approximate region employed in BMD measurement.

The institutional review board for clinical investigations at INR approved the protocol for radiation of healthy subjects and written consent was obtained from all parents and/or participants. The effective dose[22] for the complete examination was 0.34 mSv (the International Commission for Radiology Protection establishes 2 mSv as the maximum permissible public exposure level per year).

The following five normal weight groups were studied: 11 young adult girls (aged 11-22 years old, without genetic disorders and fracture history, and BMD of 187.5 ± 15.4 mg/cm^3); 14 adult women, aged 54-87 years, with an osteoporosis diagnose, very low T-score (-6.41 ± 1.04 SD); 16 DMD children with normal z-score (0.40 ± 1.10 SD); 9 DMD children with low z-score (-1.82 ± 0.68 SD); and 8 DMD with very low z-score (-3.89 ± 1.00 SD), most of them boys. All images were obtained from the PACS-INR database.

An analysis of variance and student t-test were applied to compute the probability of acceptance of the null hypothesis among the study groups. Algorithms for both image processing and statistical tests were implemented in Matlab.

Texture analysis

For texture analysis, the L3 vertebra was used as the most representative of microarchitecture changes of trabecular bone. ROIs were identified manually in the maximum possible area generating a subregion of 16 x 16 pixels (Figure 1). An interpolated subregion is shown in Figure 2 for healthy and low-BMD subjects.

There are at least three possible methods to compute the fractal dimension described in[15,16] and[17]. One of them uses the power spectrum, and the others are based on surface areas. The ones using surface areas are discarded because their method strongly depends on the image intensity during the binarization process that is needed to allow the morphological operators application.

The other two methods to quantify the bone status are by the computation of fractal dimension using power spectrum and by the computation of the energy of the first level frequency bands in wavelets packets. These methods are described below.

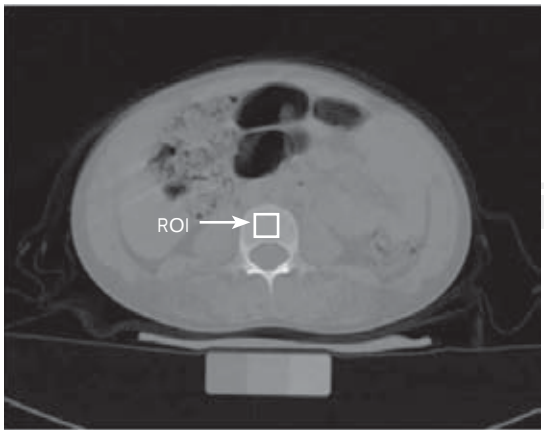

Figure 1. CT axial image of L3 vertebra with a ROI identification in the trabecular bone.

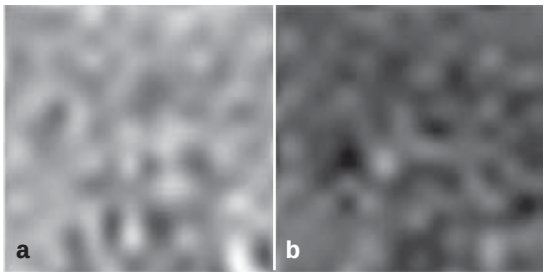

Figure 2. ROI for patients with a healthy bone (a) and with low BMD (b) with B-spline interpolation.

Computation of fractal dimension using power spectrum[16]

The power spectrum of an image was represented in polar coordinates as $PS(r,\theta)$, where r is the discrete frequency, θ is the angle of orientation on the image, and N_r is the number of data points available for each frequency r. The average power spectrum over all orientations was calculated from

$$PS(r) = \sum_{\theta=0}^{360} \frac{PS(r,\theta)}{N_r} \quad (1)$$

If an exponential relationship is considered between power and frequency,

$$PS(r) \propto \frac{1}{r^{\beta}} \quad (2)$$

by taking the logarithm we have

$$\log(PS(r)) = \log(K) - \beta\log(r) \quad (3)$$

A least squares fitted straight line between $\log(PS(r))$ and $\log(r)$ was computed, and the global fractal dimension D_{PS} was calculated from the slope β using $D_{PS} = (8-\beta)/2$. Bidimensional Fourier transform is then used to calculate the power spectrum.

Computation of frequency bands energy generated with Wavelets packets[19]

The wavelet transform, as an important multi-resolution analysis tool, has been commonly applied to texture analysis. It provides a precise and unifying framework for the analysis and characterization of a

signal at different scales. It is described as a multi-resolution analysis tool for the finite energy function $f(x) \in L2$. It can be implemented efficiently with the pyramid-structured wavelet transform and the wavelet packet transform. The pyramid-structured wavelet performs further decomposition of a signal only in the low-frequency regions. Adversely, the wavelet packet transform (WPT) decomposes a signal in all low and high frequency regions. Because the WPT describes much more spectral information than WT, a WPT is used to obtain all frequency information of a texture image.

The 2D wavelet transform can be performed by the tensor product of two 1-D base functions along the horizontal and vertical directions, and the corresponding filters can be expressed as $h_{LL}(k,l) = h(k)h(l)$, $h_{LH}(k,l) = h(k)g(l)$, $h_{HL}(k,l) = g(k)h(l)$, and $h_{HH}(k,l) = g(k)g(l)$. An image (f) can be decomposed into four sub-images by convolving the image with these filters. These four sub-images characterize the frequency information of the image in the LL, LH, HL, and HH frequency regions, respectively. The WPT repeats this process for each sub-image (Figure 3). The LH, HL and HH represent high spatial frequency components related to horizontal, vertical and diagonal image details, respectively (Figure 4).

Most of the research in multi-resolution analysis based on the wavelet domain focuses on directly extracting the energy values from the sub-images and uses them to characterize the texture image. In this work, the energy distribution of a sub-image is calculated by the squaring of the sub-image coefficients

$$e = \frac{1}{N}\sum_k |f(k)|^2$$

An Haar wavelet was used throughout the three levels of decomposition.

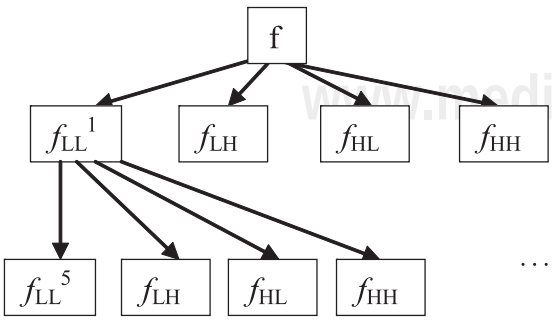

Figure 3. Tree representation of a two-level 2-D wavelet packet decomposition.

The energy of the frequency components (f_{LL}^{1}, f_{LH}^{2}, f_{HL}^{3}, f_{HH}^{4}) was calculated because they exhibited the main difference between healthy children and osteoporotic women. A spline interpolation is used.

RESULTS AND DISCUSSION

Mean and standard deviations were computed (Table 1) for the five study groups and for the five texture indicators (fractal dimension (D_{ps}) and wave-

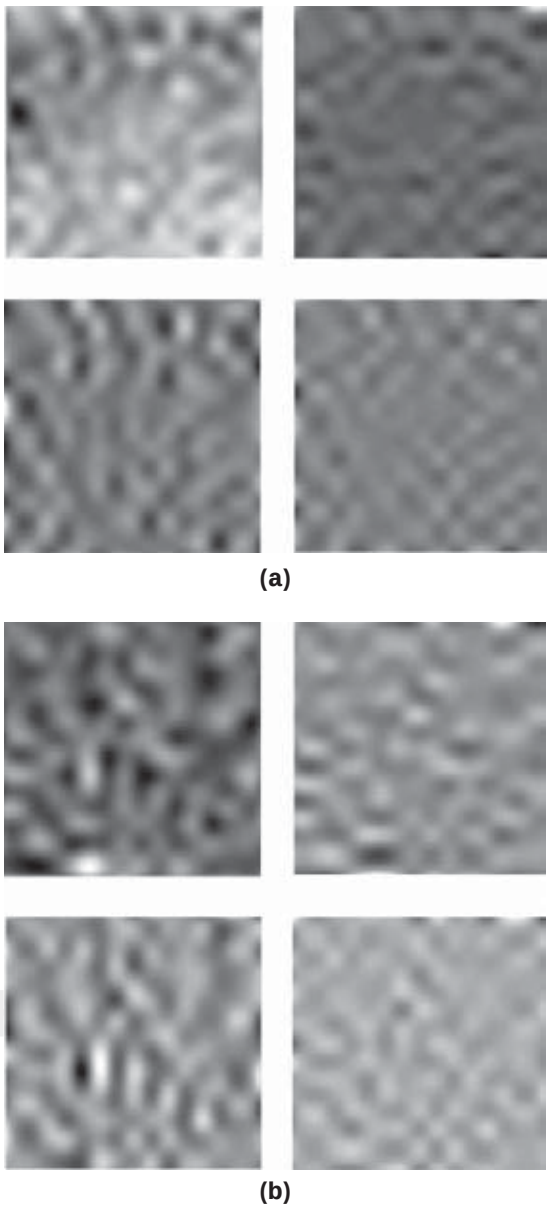

Figure 4. Approximation image (e_{LL}^{1}), horizontal (e_{LH}^{2}), vertical (e_{HL}^{3}) and diagonal (e_{HH}^{4}) sub-images, for a healthy child (a) and an osteoporotic woman (b), respectively.

Table 1. Mean and standard deviation for frequency based texture indicators and study groups.

	D_{ps}	e_{LL}^1	e_{LH}^2	e_{HL}^3	e_{HH}^4
Healthy girls	5.01 ± 0.07	18,483 ± 919	0.1943 ± 0.0647	0.1587 ± 0.0431	0.0009 ± 0.0003
Osteoporotic women	4.92 ± 0.04	16,570 ± 946	0.3073 ± 0.0601	0.2651 ± 0.0499	0.0017 ± 0.0007
DMD (normal BMD)	5.07 ± 0.09	17,869 ± 1,207	0.1065 ± 0.0476	0.1173 ± 0.0614	0.0005 ± 0.0003
DMD (low BMD)	5.05 ± 0.07	17,813 ± 1,383	0.1163 ± 0.0573	0.1312 ± 0.0476	0.0006 ± 0.0003
DMD (very low BMD)	5.01 ± 0.04	17,640 ± 1,451	0.1706 ± 0.0450	0.1664 ± 0.0285	0.0009 ± 0.0002

Table 2. P-values for a student t-test between healthy girls and osteoporotic women.

	D_{ps}	e_{LL}^1	e_{LH}^2	e_{HL}^3	e_{HH}^4
Girls	0.0004	0.0000	0.0002	0.0000	0.0000

Table 3. P-value for the analysis of variance of the 3 DMD groups.

D_{ps}	e_{LL}^1	e_{LH}^2	e_{HL}^3	e_{HH}^4
0.0175	0.7226	0.0040	0.0174	0.0025

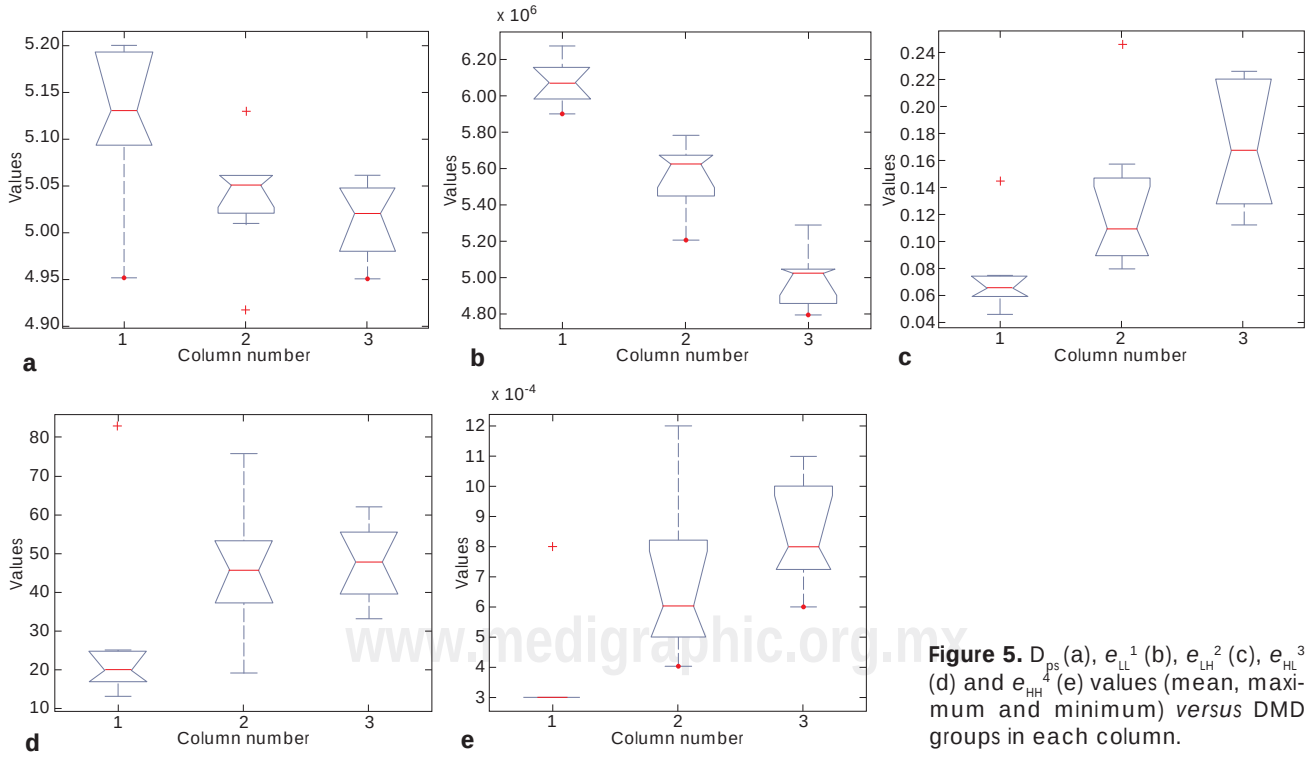

Figure 5. D_{ps} (a), e_{LL}^1 (b), e_{LH}^2 (c), e_{HL}^3 (d) and e_{HH}^4 (e) values (mean, maximum and minimum) *versus* DMD groups in each column.

let packets energy bands (e_{LL}^1, e_{LH}^2, e_{HL}^3, e_{HH}^4)).

When comparing the healthy girls group with osteoporotic women either by D_{ps} or the four WPT energy bands (Table 2), significant differences were found ($p < 0.0004$). This test demonstrates the great difference in spatial frequency components between healthy and osteoporotic subjects. For this case, D_{ps} decreases with osteoporosis (as

Table 4. P-values for a student t-test between DMD groups and osteoporotic women.

	D_{ps}	e_{LL}^1	e_{LH}^2	e_{HL}^3	e_{HH}^4
DMD (normal BMD)	0.0000	0.0000	0.0000	0.0000	0.0000
DMD (low BMD)	0.0000	0.0047	0.0000	0.0000	0.0000
DMD (very low BMD)	0.0001	0.9439	0.0001	0.0001	0.0000

previously reported), but on the contrary, energy in e_{LH}^2, e_{HL}^3, e_{HH}^4 increases as high spatial frequencies appear.

On the other hand, applying the analysis of variance among the three DMD children groups classified by their z-score as having normal, low and very low BMD, significant differences were found for almost all texture indicators ($p < 0.0175$). This test shows a relationship between the BMD decrease and an increase in high spatial frequencies for normal-weight patients (Table 3). Minimum, mean and maximum texture indicator values are shown in Figure 5.

When applying the statistical test to compare the DMD children groups with osteoporotic women, great statistical differences for all texture indicators ($p < 0.0001$) were found, with the exception of e_{LL}^1. The low WPT frequency band has a high probability of similarity with BMD due to the strong relationship with the image intensity (Table 4).

CONCLUSIONS

The main contribution of this work is the texture analysis performed to improve the diagnosis by image intensity (BMD). This issue must be taken into account when diagnosing osteoporosis in DMD children because bone mineral densities could overestimate the trabecular bone deterioration.

None of the members of the employed control groups were overweight, to diminish variance and to improve the rejection of the null hypothesis.

It was found an increase of high frequency components in osteoporotic women in comparison with those healthy girls in their peak bone mass. This may be attributed to the augment in the trabecular bone porosity.

On the other hand, this above mentioned result is confirmed with the performed analysis of variance for Duchenne muscle dystrophy patients, where it was found also a relationship between the incremental appearances of high spatial components and decreasing BMD.

However, it must be mentioned that although there is a similar z-score between DMD with very low BMD and osteoporotic women, the former did not showed as high spatial frequency components as the later. We can consider at this point, as it has been previously reported, the presence of osteopenia in DMD patients without corticosteroids intake due to the lack of weight-bearing stimulus[13].

Texture analysis showed to be useful to discriminate between the healthy group and that of the osteoporotic women. This result could be useful to confirm osteoporosis in overweight adults.

For diagnosing the bone deterioration degree in DMD patients, it is suggested the control group must be the DMD with normal BMD group.

The results could be improved by increasing the radiation dose, but this issue may be controversial to radiation protection organizations and ethics committees.

REFERENCES

1. Brunetto OH. Osteoporosis en pediatría. Revista Argentina de Endocrinología y Metabolismo 2006; 43(2): 90-108.
2. Gilsanz V, Pérez FJ, Campbell PP, Dorey FJ, Lee DC, Wren TAL. Quantitative CT reference values for vertebral trabecular bone density in children and Young adults. Radiology 2009; 250(1): 222-227.
3. van Rijn RR, van der Sluis IM, Link TM, Grampp, S, Guglielmi G, Imhof H, Glüer C, Adams JE, van Kuijk C. Bone densitometry in children: a critical appraisal. Eur Radiology 2003; 13: 700-707.
4. Bachrach LK. Editorial: Osteoporosis in children: Still a diagnostic challenge. J Clin Endocrinol Metab 2007; 92(6): 2030-2031.
5. Kalkwarf HJ, Zemel BS, Gilsanz V, Lappe JM, Horlick M, Oberfield S, Mahboudi S, Fan B, Frederik M, Winer K, Shepherd JA. The bone mineral density in childhood study: bone mineral content and density according to age, sex and race. J Clin Endocrinol Metab 2007; 92(6): 2087-2099.
6. Friecke O, Sumnik Z, Tutlewski B, Stabrey A, Remer T, Schoenau E. Local body composition is associated with gender differences of bone development at the forearm in puberty. Horm Res 2008; 70: 105-111.
7. Nohara T, Ueda M, Ohta A, Sugimoto T. Correlation of body growth and bone mineral density measured by ultrasound densitometry of the calcaneus in children and adolecents. J Exp Med 2009; 219: 63-69.

8. Uppot RN. Impact of obesity in radiology. Radiol Clin N Am 2007; 45: 231-246.
9. Schindera ST, Nelson RC, Toth TL, Nguyen GT, Toncheva GI, DeLong DM, Yoshizumi TT. Effect of patient size on radiation dose for abdominal MDCT with automatic tube current modulation: phantom study. Am J Roentgenol 2008; 190: 100-105.
10. Yanch JC. Increased radiation dose to overweight and obese patients from radiographic examinations. Radiology 2009; 252: 128-139.
11. Bothwell JE, Gordon KE, Dooley JM, MacSween J, Cummings EA, Salisbury S. Vertebral fractures in boys with Duchenne muscular distrophy. Clin Pediatr 2003; 42: 353-356.
12. Schara U, Mortier J, Mortier W. Long-Term steroid therapy in Duchenne muscular distrophy- positive results *versus* side effects. J Clin Neuromusc Dis 2001; 2: 179-183.
13. Bianchi ML, Mazzanti A, Galbiati E, Saraifoger S, Dubini A, Cornelio F, Morandi L. Bone mineral density and bone metabolism in Duchenne muscular dystrophy. Osteoporosis Int 2003; 14: 761-767.
14. Szulc P, Seeman E. Thinking inside and outside the envelopes of bone. Osteoporosis Int 2009; 20: 1281-1288.
15. Southard TE, Southard KA. Detection of simulated osteoporosis in maxillae using radiographic texture analysis. IEEE Trans Biomed Eng 1996; 43(2): 123-132.
16. Jiang C, Pitt RE, Bertram JEA, Aneshansley, DJ. Fractal-based image texture analysis of trabecular bone architecture. Med Biol Eng Comput 1999; 37: 413-418.
17. Samarabandu J, Archarya R, Hausmann E, Allen K. Analysis of bone X-rays using morphological fractals. IEEE Trans Med Imaging 1993; 12(3): 466-470.
18. Unser M. Texture classification and segmentation using wavelet frames. IEEE Trans Image Process 1995; 4(11): 1549-1560.
19. Wang ZZ, Yong JH. Texture analysis and classification with linear regression model based on wavelet transform. IEEE Trans Image Process 2008; 17(8): 1421-1430.
20. Karahaliou AN, Boniatis IS, Skiadopoulos SG, Sakellaropoulos FN, Arikidis NS, Likaki EA, Panayiotakis GS, Costaridou LI. Breast cancer diagnosis: Analyzing texture of tissue surrounding microcalcifications. IEEE Trans Inf Technol Biomed 2008; 12(6): 731-738.
21. Lewiecki EM, Gordon CM, Baim S, Binkley N, Bilezikian JP, Kendler DL, Hans DB, Silverman S, Bishop NJ, Leonard MB, Bianchi ML, Kalkwarf HJ, Langman CB, Plotkin H, Rauch F, Zemel BS. Special report on the 2007 adult and pediatric position development conferences of the international society for clinical densitometry. Osteoporosis Int 2008; 19: 1369-1378.
22. Huda W, Ogden KM, Khorasani MR. Converting dose-length product to effective dose at CT. Radiology 248: September 2008 Radiology, 248, 995-1003.